Available online at www.sciencedirect.com

ScienceDirect

Ceramics International 40 (2014) 4889–4895

CERAMICS INTERNATIONAL

www.elsevier.com/locate/ceramint

Synthesis, structural and luminescence properties of Ti co-doped $ZnO/Zn_2SiO_4:Mn^{2+}$ composite phosphor

P.V. Ramakrishna*, D.B.R.K. Murthy, D.L. Sastry

Department of Physics, Andhra University, Visakhapatnam 530003, India

Received 11 August 2013; received in revised form 9 October 2013; accepted 15 October 2013
Available online 29 October 2013

Abstract

Titanium co-doped $ZnO/Zn_2SiO_4:Mn^{2+}$ (TZZM) composite phosphor was prepared by the high temperature solid state reaction method. The structural and optical properties of the as-prepared samples were analysed by means of the technique of X-ray diffraction (XRD), Scanning electron microscopy (SEM), Fourier transform infrared (FTIR) and Photoluminescence (PL) spectroscopy techniques. XRD analysis confirms the formation of ZnO/Zn_2SiO_4 composite system. The strain acting on the system was estimated using Williams–Hall plot. SEM recordings showed a distribution of ZnO and Zn_2SiO_4 particles of sizes ~1–5 μm. The luminescence properties are studied using 266 nm and 355 nm laser excitation. Results demonstrate the ability to tune the emission colour coordinates and the correlated colour temperature (CCT). This phosphor can be potentially used for optical display applications.

Keywords: Optical properties; Composite phosphor; Strain; CIE colour coordinates

1. Introduction

Mn^{2+} doped Zn_2SiO_4 phosphor is well known for its green emission (~525 nm) which arises from $^4T_1(^4G) \rightarrow {}^6A_1(^6S)$ electronic transition of Mn^{2+} ion [1]. These materials are extensively used in coatings of cathode ray tube screens (CRT), field emission displays (FEDs), plasma display panels (PDPs) and try-color lamps, due to high brightness, wide horizontal/vertical view angles, good contrast, high efficiency with a low power consumption and short response time. The FEDs are extensively used in market [2,3]. Silicate based oxide phosphor materials are more stable as compared to sulfide based phosphor like. Y_2O_2S:Eu, Gd_2O_2S:Tb, etc. Development of phosphors which show high quantum efficiency and good stability under excitation with low-voltage (≤ 5 kV) and high current density (10–100 mA/cm^2) is an important task for the scientific community [4,5]. Zn_2SiO_4 is an excellent host material due to its high refractive index (~1.7) and large band gap (~5.5 eV) [6,7]. ZnO is well known for its direct band gap ~3.3 eV. Its optical properties are significantly changed by changing the reaction conditions (temperature, pH, etc). ZnO shows luminescence in the visible range (~400–700 nm) in blue, green and red regions due to defects created [8–10]. Moreover, its band gap can be slightly tuned due to incorporation of divalent ions in Zn^{2+} sites. The combination of such interesting materials one having low band gap (ZnO) and the other having high band gap (Zn_2SiO_4), significantly improves the luminescence properties of the composite materials [11,12]. ZnO has hexagonal (wurtzite) crystal structure and lattice parameters are a=3.25 Å and c=5.12 Å. Zn atoms are tetrahedrally coordinated to four O atoms, where the d-electrons of Zn hybridize with the p-electrons [13] and TiO_2 is a semiconductor well known for its wide band gap ~3.2 eV [14]. The ionic radius of Zn^{2+}, Mn^{2+}, Si^{4+}, Ti^{4+} ions are found to be 0.06, 0.042, 0.026 nm, 0.06 nm, respectively [15]. $Zn_2SiO_4:Mn^{2+}$ has been generally prepared by solid state reaction method (SSR) for a long time [16]. Recently, Lin et al. [17] prepared Ti doped Zn_2SiO_4 thin film phosphor. Samples show good transparency of more than 80% and exhibit amorphous nature up to 800 °C.

A broad luminescence band was observed between 370 and 415 nm after annealing the sample at 700 °C. It is also reported

*Corresponding author. Tel.: +91 9949619397.
E-mail addresses: rkpuligadda@gmail.com, ramkiphysics@gmail.com (P.V. Ramakrishna).

0272-8842/$ - see front matter © 2013 Elsevier Ltd and Techna Group S.r.l. All rights reserved.
http://dx.doi.org/10.1016/j.ceramint.2013.10.065

that the photoluminescence properties are enhanced on co-doping Zn_2SiO_4:Mn^{2+} with other ions like Mg^{2+} or Cr^{3+} or Al^{3+} or Y^{3+} or Li^{+}, etc. [18]. Wang and his co-workers found significant enhancement in green emission Zn_2SiO_4:Mn^{2+} co-doped with Y^{3+}/Li^{+} due to excitation of Y–O charge transfer band (~147 nm) there by transferring energy to excited state of Mn^{2+} ion. Zn_2SiO_4 is also known to have a strong excitation band ranging from 200 to 300 nm which is supposed to arise from Mn^{2+}–O^{2+} charge transfer band (Mn–O CTB) [19]. Enhancement in emission intensity on excitation of Mn–O CTB is less expensive than UV excitation at ~147 nm. Efforts are also made to improve the luminescence efficiency of inorganic phosphor like YPO_4:Eu^{3+} or $CaMoO_4$:Tb^{3+} by co-doping with Li^{+} ions, [20–24].

In this paper, we report the work carried out on Ti co-doped ZnO/Zn_2SiO_4:5 at.% Mn^{2+} (Ti=0, 1, 3, 5, 7, 10, 15, 20 and 30 at.%) composite phosphors in which their luminescence properties are studied under 266 and 355 nm laser excitations. In addition, strain acting on the composite phosphors for different Ti co-doping was estimated.

2. Experimental section

2.1. Materials

Zinc nitrate ($Zn(NO_3)_2$, 99%), Silicon oxide (SiO_2, 99.9%), Manganese acetate ($Mn(CH_3COO)_2$, 99.9%) and (TiO_2, 99.9%) were used as starting materials.

2.2. Synthesis of Ti doped ZnO/Zn_2SiO_4:Mn composite phosphor (TZZM)

Ti co-doped ZnO/Zn_2SiO_4:5 at.% Mn^{2+} (Ti=0, 1, 3, 7, 10, 15, 20 and 30 at.%) (TZZM) phosphors were prepared using the solid-state reaction method [25]. In a typical preparation stoichiometric amounts of $Zn(NO_3)_2$, SiO_2, $Mn(CH_3COO)_2$ and TiO_2 were mixed in an agate mortar and grinded for 6–8 h for uniform mixing. This homogenous mixture was transferred to an alumina crucible and calcined at 1100 °C for 2 h. It was again grinded for 1–2 h and the calcination process was repeated at 1100 °C for 2 h. Similarly, it was repeated for different Ti co-doped ZnO/Zn_2SiO_4:5 at.% Mn^{2+} composite phosphors (Ti=0, 1, 3, 7, 10, 15, 20 and 30 at.%). These samples were subjected to X-ray diffraction (XRD), scanning electron microscope (SEM) and photo luminescence (PL) studies.

Structure and phase of the powdered samples of the composite phosphor samples were identified with the help of X-ray diffraction (XRD) patterns which were recorded on PW 1071 Philips powder X-ray diffractometer using Ni filtered Cu-Kα (1.5405 Å) radiation and operated at 30 kV and 15 mA. SEM images of the samples were recorded by employing a Philips XL 30 ESEM scanning electron microscope (FEI-Philips Company, Hillsboro). Fourier transform infrared (FTIR) spectra of the samples were recorded by Spectrum RX-I spectrophotometer (Perkin Elmer). For the photo luminescence (PL) measurement, Nd:YAG laser (266, 355 nm/Spitlight 600, Innolas) was used as an excitation source. All the emission spectra were recorded with iHR320 imaging spectrometer at room temperature.

3. Results and discussions

3.1. XRD and SEM analysis

XRD patterns of TZZM composite phosphor (Ti=0, 3, 10 and 30 at.%) with corresponding JCPDS stick plots for ZnO Card no. (36-1451) and Zn_2SiO_4 Card no. (37-1485) are show in Fig. 1. It is evident from XRD patterns that the samples have both ZnO and Zn_2SiO_4 phases. It is observed from the intensity of XRD patterns without Ti concentration (0 at.%) ZnO phase is dominant as compared to Zn_2SiO_4 phase diffraction peaks with Ti^{4+} doping. As Ti^{4+} concentration is increases the amount of ZnO phase decreases while the amount of Zn_2SiO_4 phase increases in the TZZM composite phosphor. For 30 at.% Ti co-doped samples it can be seen that Zn_2SiO_4 becomes the main phase whereas ZnO becomes a minor phase. It is probably because TiO_2 which is isovalent with SiO_2 is favouring the formation of Zn_2SiO_4 as compared to ZnO [26]. Fig. 2 shows the comparison of XRD patterns of 0, 3, 10 and 30 at.% Ti co-doped TZZM composite phosphor in 2θ range from 33.5° to 37°. The intensity of (101) diffraction peak of ZnO decreases whereas the intensity of (410) diffraction peak of Zn_2SiO_4 increases with the increase in Ti co-doping. Moreover, the XRD peak position of ZnO phase almost remains unchanged with the increase in Ti ion concentration while there is a small shift

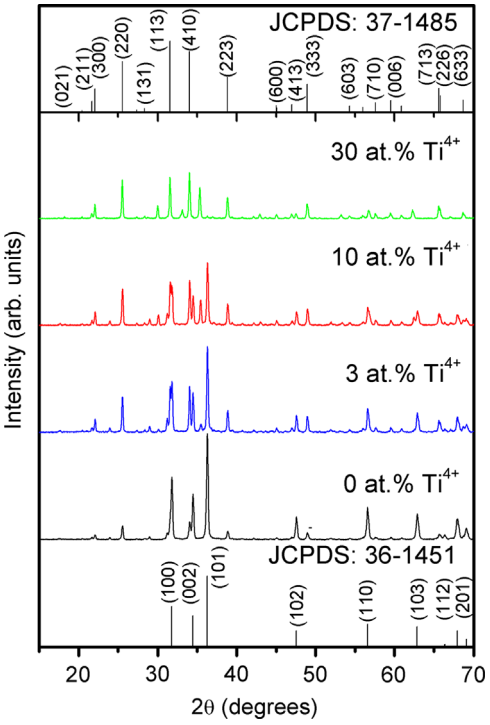

Fig. 1. XRD patterns of 0, 3, 10 and 30 at.% Ti co-doped TZZM composite phosphor. Here some selected planes from JCPDS Card nos.: 36-1451 (ZnO) and 37-1485 (Zn_2SiO_4) are shown for clarity.

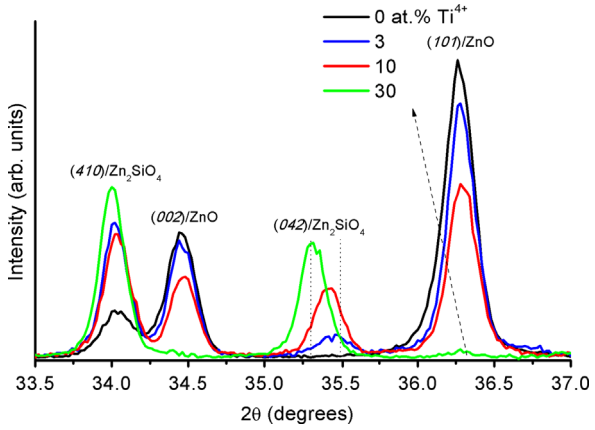

Fig. 2. Comparison of XRD patterns of 0, 3, 10 and 30 at.% Ti co-doped TZZM composite phosphor.

to lower angle by ~0.2° in the peak position of Zn_2SiO_4 phases. This may be due to the difference in ionic radius of Si^{4+} (0.026 nm) and Ti^{4+} ion (0.06 nm), i.e., for Zn_2SiO_4 phase lattice expansion may be expected as Ti^{4+} goes in to the position of Si^{4+} and for ZnO phase unit cell volume is almost unaffected, indicating Ti^{4+} does not occupy Zn site. This confirms that Ti^{4+} ions occupy the Si^{4+} sites. However it can be expected that Mn^{2+} ion occupy Zn^{2+} sites in both ZnO and Zn_2SiO_4. Since both Zn and Mn are divalent and their ionic radii (0.06 and 0.042 nm) are comparable. Recently, Hao et al. reported similar results in the case of $Zn_{1.92-x}Ba_xSi_{1-y}Ti_yO_4$:0.08$Mn^{2+}$ samples in which Mn ion occupied Zn sites and Ti ion occupies the Si sites [27].

The Scherer relation given in Eq. (1) is used to calculate the average crystallite size from XRD patterns [28].

$$D = \frac{0.9\lambda}{\beta_{hkl}\cos\theta} \tag{1}$$

λ is the wavelength of the X-ray and β_{hkl} is the full width at half maximum (FWHM) of peak of the XRD pattern. Strain developed in nanoparticles is calculated using Williams–Hall equation which can be expressed as follows:

$$\frac{\beta_{hkl}\cos\theta}{\lambda} = \frac{1}{D} + (\varepsilon)\frac{\sin\theta}{\lambda} \tag{2}$$

where θ is the Bragg angle of (h,k,l) diffraction, β_{hkl} the FWHM of the (h,k,l) diffraction peak, λ the X-ray wavelength, D the effective crystallite size, and ε the strain developed in the lattice [28].

The average crystallite sizes calculated using the FWHM of the maximum intensity diffraction peak (101) of ZnO are found to be ~41, 46 and 48 nm for 0, 3 and 10 at.% Ti doped samples, respectively. Plot of Williams–Hall equation for 0, 3, 10 and 30 at.% Ti co-doped TZZM composite phosphor is shown in Fig. 3 in which $\beta_{hkl}\cos\theta/\lambda$ vs $\sin\theta/\lambda$ is plotted for diffraction peaks corresponding to Zn_2SiO_4 phase. The linear plot shows a positive slope. The strain (ε_{hkl}) increases with Ti ion co-doping and varies between 40 and 59 ($\times 10^{-4}$).

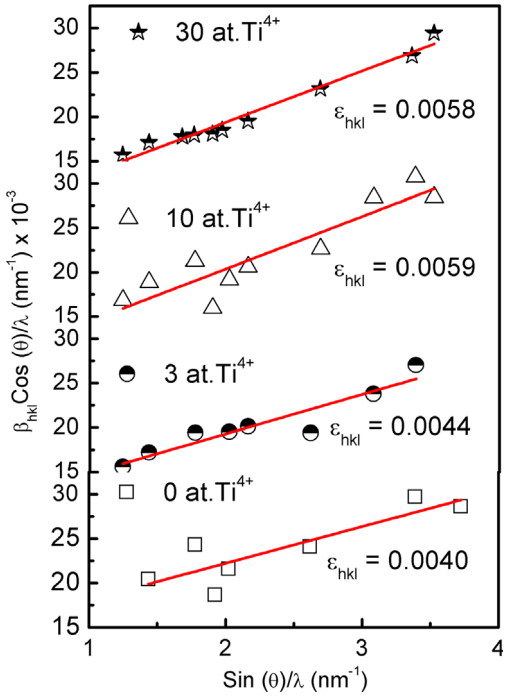

Fig. 3. Plot of Williams–Hall equation for 0, 3, 10 and 30 at.% Ti co-doped TZZM composite phosphor.

The SEM micrographs of 1 and 30 at.% Ti co-doped TZZM samples are shown in Fig. 4. The surface morphology indicates good grain growth with shape anisotropy and it clearly shows the presence of two types of phases in the structure. The grains of unequal size are distributed throughout the sample. The average grain size (d ~ 1–5 μm) has been evaluated by using the linear intercept method by the relation

$$d = 1.56\frac{L}{MN} \tag{3}$$

where L is the random line length, M the magnification of image and N the number of grain-boundary intercepts by the line. However, sizes of the particles are larger as compared to the XRD analysis.

3.2. FTIR analysis

FTIR spectra of ZnO/Zn_2SiO_4:5 at.% Mn^{2+} with and without Ti^{4+} co-doping were recorded. Fig. 5 shows the FTIR spectra of 5 at.% Ti co-doped TZZM composite phosphor and without Ti co-doped spectra is shown in Fig. S1 (Supplementary data). The spectra give a clear indication of the groups present in the sample. The spectrum was recorded in the wavelength range 4000–400 cm^{-1}. There is a broad peak at 3442 cm^{-1} which can be assigned to the symmetric stretching vibrations of O–H group [20]. It indicates the presence of –OH groups absorbed by the sample from the atmosphere. FTIR spectra also show two strong peaks centered around ~931 and 577 cm^{-1} which can be assigned to searching of Si–O and Zn–O bonds in SiO_4 and ZnO_4 tetrahedra in the host, respectively [25]. It can be seen that the intensity of Si–O

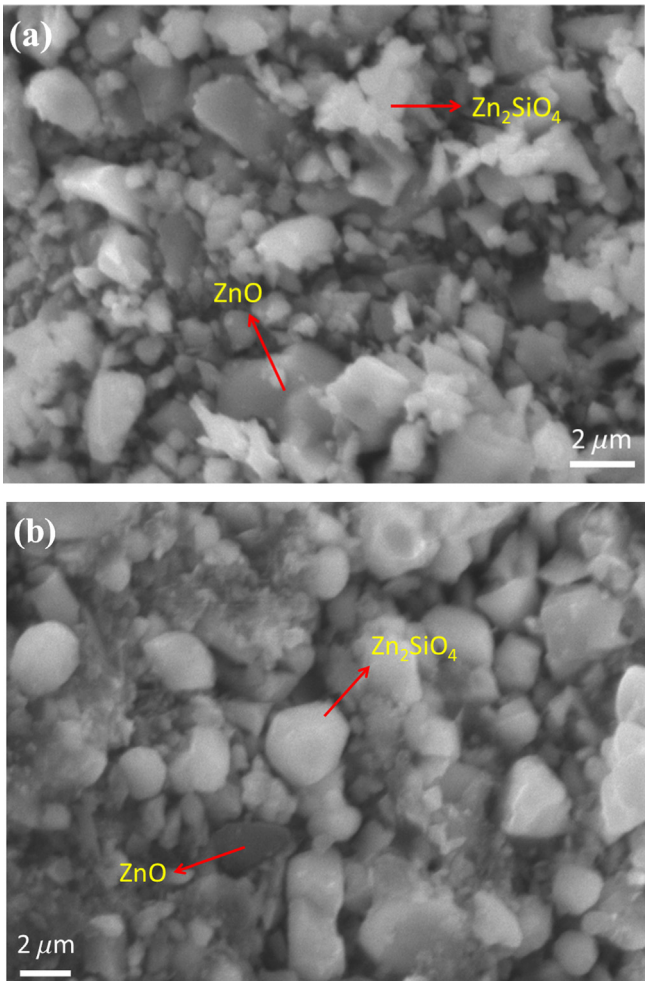

Fig. 4. The SEM image of (a) 1 at.% Ti and (b) 30 at.% Ti doped ZnO/Zn_2SiO_4 sample.

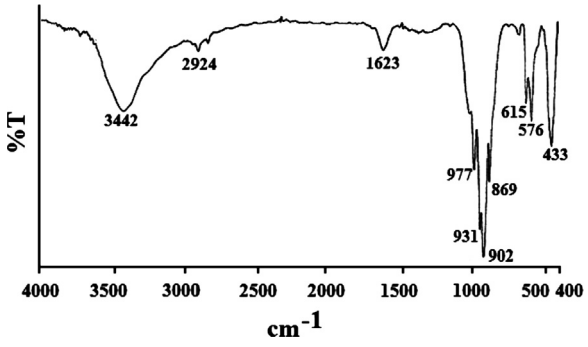

Fig. 5. FTIR spectra of 5 at% Mn ZnO/Zn_2SiO_4 composite phosphor.

stretching band is significantly higher than Zn–O stretching band.

The vibrations at 977, 931 and 902 cm^{-1} correspond to asymmetric stretching vibration modes (v_3-SiO_4), whereas 869 cm^{-1} is due to symmetric stretching vibration mode (v_1-SiO_4). The two vibrations at 615 and 576 cm^{-1} are assigned to asymmetric (v_3-ZnO_4) and symmetric (v_1-ZnO_4) mode of vibrations, respectively [25]. It is observed that symmetric vibration intensity is slightly higher than asymmetric vibration with in ZnO_4 group which is opposite to that observed for SiO_4 group. The observation of IR bands corresponding to both ZnO_4 and SiO_4 tetrahedra confirm the formation of Zn_2SiO_4 phase. The peaks at 433 cm^{-1} is present only in Ti co-doped sample (Fig.5) and is assigned to Ti–O–Ti vibrations [25]. It is further confirmed by FTIR spectrum of Ti undoped samples (Fig. S1).

3.3. Luminescence analysis

Fig. 6 shows the photoluminescence spectra of the composite phosphor under 266 nm (~4.6 V) laser excitation. It can be clearly seen that there are three transitions peaks centered around ~400, 530 and 794 nm. The luminescence peak around 530 nm is more dominant when compared to other peaks. Emission peaks centered around ~400 nm (3.1 eV) and 794 nm (1.56 eV) are related to surface/oxygen defects in ZnO crystals [29,30]. In general it is reported in the literature that a peak centered between ~380 and 395 nm is observed due to the recombination of free excitions through an exciton–exciton collision process nearer to the band gap and is assigned to band edge emission in ZnO [30]. This peak is not observed here. The surface defect emission around ~400 nm between 377 and 455 nm has full width at half maximum (FWHM) of ~19 nm for 7 at.% Ti co-doped samples. FWHM initially increases with Ti co-doping up to 7 at.% and then decreases. This peak is more symmetric at lower wavelength side and is asymmetric at higher wavelength side. Deconvoluted spectrum of 7 at.% Ti co-doped sample between 380 and 450 nm using Gaussian function is shown in Fig. 7(a). Two peaks at ~400 and 415 nm are observed to fit very well to the experimental spectrum having goodness of fitting χ^2=0.9916. Other fitting parameters are shown in the figure itself. Gaussian fitting to emission spectrum between 770 and 815 nm is shown in Fig. 7 (b) showing a peak centered at ~795 nm with FWHM of ~21.5 nm. It is observed that the emission intensity at 400 nm is ~7 times higher than emission intensity at 795 nm. Also some small peaks are observed at ~686, 698 and 709 nm which are defect-related emissions from ZnO. Their intensity is very weak as compared to the other peaks. In addition to

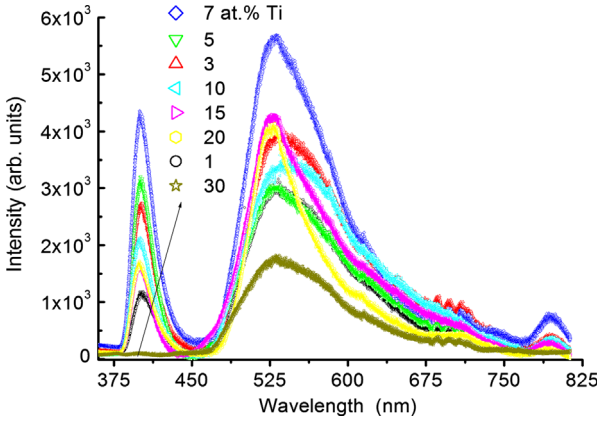

Fig. 6. Luminescence spectra of Ti co-doped TZZM composite phosphor under 266 nm laser excitation.

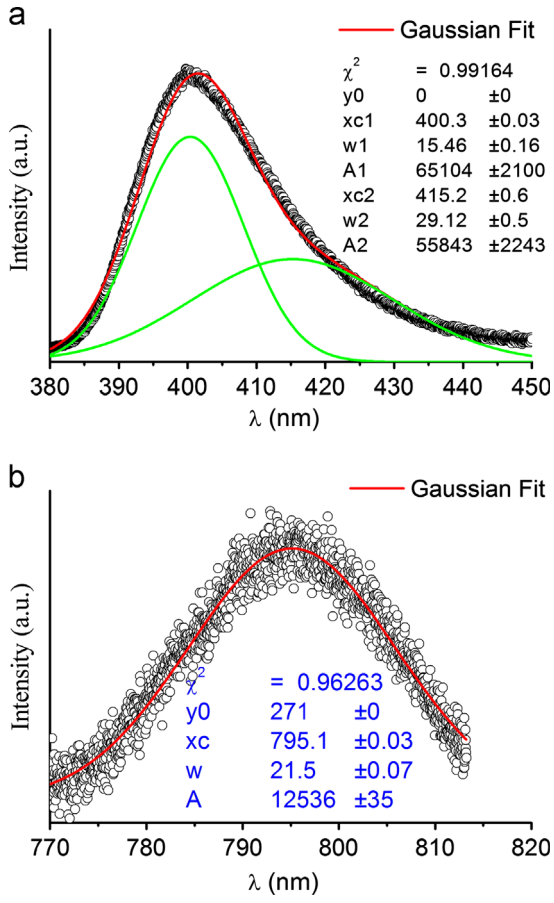

Fig. 7. (a) Deconvoluted spectrum of 7 at.% Ti co-doped sample between 380 and 450 nm using Gaussian function, (b) Gaussian fitting to emission spectrum between 770 and 815 nm, fitting parameters are shown in the corresponding figures itself.

ultraviolet (UV) emission due to its band gap (edge emission) ZnO has emission peaks in blue, green, yellow and red regions of the visible spectrum. Bano et al. have grown ZnO nanorods on a plastic substrate which shows UV, green and red emissions peaks between 350 and 750 nm [31]. Similar defect emissions are discussed in detailed in a review by Willander et al. [32] The broad peak between 450 and 750 nm (Fig. 6) centered at 523 nm is assigned to $^4T_1(^4G) \rightarrow {}^6A_1(^6S)$ transition of Mn^{2+}. Recently, Kakihana and his co-workers prepared Mn doped Zn_2SiO_4 by solid state and polyol modified method in which samples show emission peaks centered at ~523 nm, which match well with those reported in TZZM composite phosphor [33]. It is also observed that the peak shows asymmetric nature in higher wavelength side and is symmetric in lower wavelength side. This may be due to the overlap of defect emission from ZnO with the emission from Mn^{2+} doped Zn_2SiO_4 [31]. On deconvolution of the emission spectrum of 7 at.% Ti co-doped sample between 468 and 670 nm using Gaussian function, two peaks centered at ~523 and 570 nm are observed to be clearly resolved (which is not shown here). It is found that the emission intensity of composite phosphor increases with Ti co-doping up to a concentration of 7 at.% and then decreases. The branching ratio (β) of the emission between 375 and 815 nm is calculated by assuming the intensity of emission peaks at ~400, 523, 570 and 795 nm as 100% for 1 and 7 at.% Ti co-doped composite phosphor samples. The β values are found to be 6%, 40.9%, 52% and 1.1% for 1 at.% Ti co-doping and 16.7%, 30.8%, 50.3% and 2.3% for 7 at.% Ti co-doping. On increasing Ti co-doping concentration there is a significant enhancement in emission intensity at ~400 nm. Moreover, broadening arises in the peak around 523 nm due to overlapping of prominent green emission (~523 nm) from Mn^{2+} ion and a broad emission (~570 nm) due to ZnO defect. Hence it is very difficult to compare emission intensity from branching ratio.

The steady state emission spectra of composite phosphor for different concentration of Ti co-doping were obtained under 355 nm (~3.5 eV) laser excitation between 370 and 900 nm range and are presented in Fig. 8. The sharp emission around ~400 nm and the broad emissions peaks around ~540 and 707 nm are related to surface/oxygen defects in ZnO host [29,30]. It is found that the emission intensity increases with Ti co-doping. Inset of Fig. 8 shows the variation in integrated emission intensity between 370 and 900 nm with different

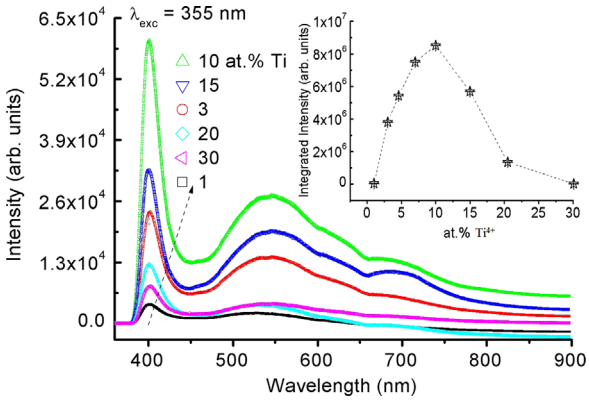

Fig. 8. Luminescence spectra of Ti co-doped TZZM composite phosphor under 355 nm laser excitation.

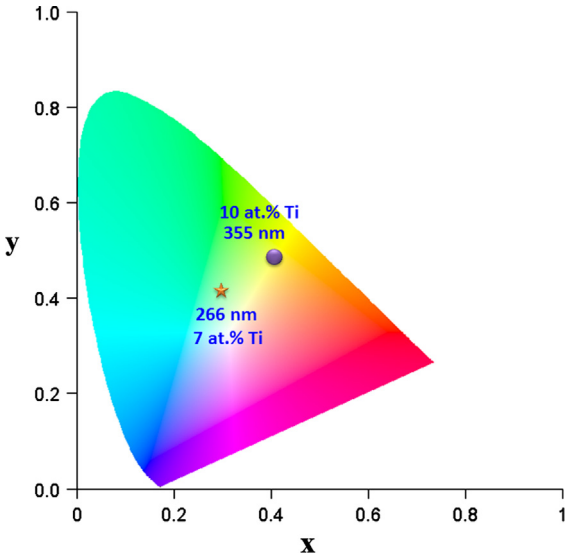

Fig. 9. CIE coordinates for 7 and 10 at.% Ti co-doped composite phosphor under 266 and 355 nm laser excitations.

Table 1
The calculated CIE chromaticity coordinates and CCT values (K) of the ZnO/Zn_2SiO_4/5 at% Mn composite phosphor for different concentration (at.%) of Ti co-doping.

Ti at%	CIE coordinates						
	$\lambda_{ex}=266$ nm			$\lambda_{ex}=355$ nm			
	x	y	CCT (K)	Ti at%	x	y	CCT (K)
1	0.4337	0.4572	3675	1	0.2693	0.4171	7994
3	0.4389	0.4566	3532	3	0.3039	0.4493	6961
5	0.4357	0.4625	3692	5	0.3020	0.4301	7012
7	0.4263	0.4514	3794	7	0.3015	0.4343	7024
10	0.4488	0.4644	3385	10	0.3010	0.4346	7038
15	0.4315	0.4634	3809	15	0.3138	0.4735	6743
20	0.432	0.4673	3844	20	0.2665	0.3883	8276
30	0.4217	0.4516	3918	30	0.2994	0.4381	7080

concentration of Ti co-doping. Optimum emission is found for 10 at.% of Ti co-doping samples. It can be clearly observed that the emission intensity at 400 nm is greater than emission intensity 540 nm which is greater than emission intensity at 707 nm. Similar results were observed in case of ZnO [31]. Fig. 9 shows the Commission Internationale de l'Eclairage (CIE) chromaticity coordinates for composite phosphor samples for 7 and 10 at.% Ti co-doped concentrations under 266 and 355 nm laser excitation. The CIE coordinates are very close to (0.43, 0.45) for 266 nm laser excitation and their values are slightly shifted around (0.3, 0.43) under 355 nm laser excitations. The correlated color temperature is calculated using McCamy empirical formula in terms of CCT values, which is expressed as [34]

$$\mathrm{CCT} = -499n^3 + 3525n^2 - 6823n + 5520.33 \quad (4)$$

where $n=(x-x_e)/(y-y_e)$ is the inverse slope line, $x_e=0.332$ and $y_e=0.186$. The CCT values for 7 and 10 at.% Ti co-doped samples are found to be 3794 and 7038 K, for 266 and 355 nm excitations, respectively. The CCT values of the samples slightly vary with Ti co-doping under 266 and 355 nm excitations. CIE coordinate and CCT values for different Ti co-doped samples are shown in Table 1 for 266 and 355 nm laser excitations.

4. Conclusions

In summary, we have synthesized a series of Ti co-doped ZnO/Zn_2SiO_4:5 at.% Mn^{2+} composite phosphor (TZZM) using the solid state reaction method. It is found that the strain values vary in between ~0.0040 and 0.0059. It is interesting that Ti^{4+} ions which occupying Si^{4+} sites in Zn_2SiO_4 are found to be not only affecting the PL spectra of Zn_2SiO_4:5 at.% Mn^{2+} phase but also those of ZnO phase in the ZnO/Zn_2SiO_4:5 at.% Mn^{2+} composite phosphor co-doped with Ti^{4+}. The particle size measured from SEM is greater than that obtained from XRD analysis. The CIE coordinates are very close to (0.43, 0.45) for 266 nm laser excitation and its values are slightly shifted to around (0.30, 0.43) under 355 nm laser excitations. The CCT values for 7 and 10 at.% Ti co-doped samples are found to be 3794 and 7038 K, for 266 and 355 nm excitations, respectively. The CCT values are found to be slightly dependent on Ti^{4+} co-doped ion concentration. This phosphor can be potentially used for optical display applications.

Appendix A. Supporting information

Supplementary data associated with this article can be found in the online version at http://dx.doi.org/10.1016/j.ceramint.2013.10.065.

References

[1] S. Zhang, M. Lu, Y. Li, F. Sun, J. Yang, S. Wang, Synthesis and electrochemical properties of Zn_2SiO_4 nano/mesorods, Mater. Lett. 100 (2013) 89.
[2] M. Shang, G. Li, D. Yang, X. Kang, C. Peng, Z. Cheng, J. Lin, $(Zn, Mg)_2GeO_4:Mn^{2+}$ submicrorods as promising green phosphors for field emission displays: hydrothermal synthesis and luminescence properties, Dalton Trans., 40, , 2011, p. 9379.
[3] M. Takesue, H. Hayashi, R.L.S. Jr, Thermal and chemical methods for producing zinc silicate (willemite): a review, Prog. Cryst. Growth Charact. Mater. 55 (2009) 98.
[4] G. Li, D. Geng, M. Shang, C. Peng, Z. Cheng, J. Lin, Tunable luminescence of Ce^{3+}/Mn^{2+}-coactivated $Ca_2Gd_8(SiO_4)_6O_2$ through energy transfer and modulation of excitation: potential single-phase white/yellow-emitting phosphors, J. Mater. Chem. 21 (2011) 13334.
[5] V.A. Bolchouchine, E.T. Goldburt, B.N. Levonovitch, V.N. Litchmanova, N.P. Sochtine, Designed, highly-efficient FED phosphors and screens, J. Lumin. 87–89 (2000) 1277.
[6] M.J. Weber, Hand Book of Optical Materials, CRC Press, USA, 2003.
[7] X. Feng, X. Yuan, T. Sekiguchi, W. Lin, J. Kang, Aligned $Zn-Zn_2SiO_4$ core−shell nanocables with homogenously intense ultraviolet emission at 300 nm, J. Phys. Chem. B 109 (2005) 15786.
[8] A.K. Singh, V. Viswanath, V.C. Janu, Synthesis, effect of capping agents, structural, optical and photoluminescence properties of ZnO nanoparticles, J. Lumin. 129 (2009) 874.
[9] M. Ghosh, A.K. Raychaudhuri, Shape transition in ZnO nanostructures and its effect on blue-green photoluminescence, Nanotechnology 19 (2008) 445704.
[10] M. Abdullah, T. Morimoto, K. Okuyama, Generating blue and red luminescence from ZnO/poly(ethylene glycol) nanocomposites prepared using an in-situ method, Adv. Funct. Mater. 13 (2003) 800.

[11] L.E. Mir, A. Amlouk, C. Barthou, S. Alaya, Synthesis and luminescence properties of ZnO/Zn_2SiO_4/SiO_2 composite based on nanosized zinc oxide-confined silica aerogels, Physica B 388 (2007) 412.
[12] X. Wang, C.J. Sumers, Mesoporous single crystal ZnO nano wires epitaxially sheated with Zn_2SiO_4, Adv. Mater. 16 (2004) 1215.
[13] Y.W. Heo, K. Ip, S.J. Pearton, D.P. Norton, The near band-edge emission and photoconductivity response of phosphorus-doped ZnO thin films grown by pulsed laser deposition, Phys. Status Solidi A 201 (2004) 1500.
[14] R.S. Ningthoujam, V. Sudarsan, S.V. Godbole, L. Kienle, S. K. Kulshreshtha, A.K. Tyagi, SnO_2:Eu^{3+} nanoparticles dispersed in TiO_2 matrix: improved energy transfer between semiconductor host and Eu^{3+} ions for the low temperature synthesized samples, Appl. Phys. Lett. 90 (2007) 173113.
[15] R. Shannon, C. Prewitt, Effective ionic radii in oxides and fluorides, Acta Crystallogr. Sect. B Struct. Crystallogr. Cryst. Chem. 25 (1969) 925.
[16] G. Blasse, B.C. Grabmaier, Luminescent Materials, Springer, New York, 1994.
[17] C. Lin, Y. Lai, J. Chen, Photoluminescence behavior of Ti-doped Zn_2SiO_4 thin film phosphors, ECS Trans. 1 (34) (2006) 1–6.
[18] J. Liu, Y. Wang, X. Yu, J. Li, Enhanced photoluminescence properties of Zn_2SiO_4:Mn^{2+} co-activated with Y^{3+}/Li^+ under VUV excitation, J. Lumin. 130 (2010) 2171.
[19] V. Bhatkar, S. Omanwar, S. Moharil, Combustion synthesis of the Zn_2SiO_4:Mn phosphor, Phys. Status Solidi A 191 (2002) 272.
[20] A.K. Parchur, R.S. Ningthoujam, Preparation, microstructure and crystal structure studies of Li^+ co-doped YPO_4:Eu^{3+}, RSC Adv. 2 (2012) 10854.
[21] A.K. Parchur, A.I. Prasad, S.B. Rai, R. Tewari, R.K. Sahu, G.S. Okram, R.A. Singh, R.S. Ningthoujam, Observation of intermediate bands in Eu^{3+} doped YPO_4 host: Li^+ ion effect and blue to pink light emitter, AIP Adv. 2 (2012) 032119.
[22] G.S.R. Raju, E. Pavitra, Y.H. Ko, J.S. Yu, A facile and efficient strategy for the preparation of stable $CaMoO_4$ spherulites using ammonium molybdate as a molybdenum source and their excitation induced tunable luminescent properties for optical applications, J. Mater. Chem. 22 (2012) 15562.
[23] A.K. Parchur, R.S. Ningthoujam, Behaviour of electric and magnetic dipole transitions of Eu^{3+}, 5D0→7F0 and Eu–O charge transfer band in Li^+ co-doped YPO_4:Eu^{3+}, RSC Adv. 2 (2012) 10859.
[24] A.K. Parchur, A.I. Prasad, A.A. Ansari, S.B. Rai, R.S. Ningthoujam, Luminescence properties of Tb^{3+}-doped $CaMoO_4$ nanoparticles: annealing effect, polar medium dispersible, polymer film and core–shell formation, Dalton Trans. 41 (2012) 11032.
[25] S.D. Ross, Inorganic Infrared and Raman Spectra, McGraw-Hill, New York, 1972.
[26] F.A. Cotton, G. Wilkinson, C.A. Murillo, M. Bochman, Advance Inorganic Chemistry, 6th edition, Wiley-Blackwell, Wiley Interscience, New York, 1999.
[27] Y. Hao, L. Song, Y. Wang, Luminescence properties and mechanism of $Zn_{1.92-x}Ba_xSi_{1-y}Ti_yO_4$:0.08$Mn^{2+}$ phosphors in VUV region, J. Lumin. 131 (2011) 1605.
[28] A.K. Parchur, R.S. Ningthoujam, Preparation and structure refinement of Eu^{3+} doped $CaMoO_4$ nanoparticles, Dalton Trans. 40 (2011) 7590.
[29] L.R. Singh, R.S. Ningthoujam, S.D. Singh, Tuning of ultra-violet to green emission by choosing suitable excitation wavelength in ZnO: quantum dot, nanocrystals and bulk, J. Alloy. Compd. 487 (2009) 466.
[30] X. Teng, H. Fan, S. Pan, C. Ye, G. Li, Abnormal photoluminescence of ZnO thin film on ITO glass, Mater. Lett. 61 (2007) 201.
[31] N. Bano, S. Zaman, A. Zainelabdin, S. Hussain, I. Hussain, O. Nur, M. Willander, ZnO-organic hybrid white light emitting diodes grown on flexible plastic using low temperature aqueous chemical method, J. Appl. Phys. 108 (2010) 043103.
[32] M. Willander, O. Nur, Q.X. Zhao, L.L. Yang, M. Lorenz, B.Q. Cao, J.Z. Pérez, C. Czekalla, G. Zimmermann, M. Grundmann, A. Bakin, A. Behrends, M. Al-Suleiman, A. El-Shaer, A.C. Mofor, B. Postels, A. Waag, N. Boukos, A. Travlos, H.S. Kwack, J. Guinard, D.L.S. Dang, Zinc oxide nanorod based photonic devices: recent progress in growth, light emitting diodes and lasers, Nanotechnology 20 (2009) 332001.
[33] K. Yoshizawa, H. Kato, M. Kakihana, Synthesis of Zn_2SiO_4:Mn^{2+} by homogeneous precipitation using propylene glycol-modified silane, J. Mater. Chem. 22 (2012) 17272.
[34] A.K. Parchur, A.I. Prasad, S.B. Rai, R.S. Ningthoujam, Improvement of blue, white and NIR emissions in YPO_4:Dy^{3+} nanoparticles on co-doping of Li^+ ions, Dalton Trans. 41 (2012) 13810.